Sawtooth structure in tunneling probability for a periodically perturbed rounded-rectangular potential

Kin'ya Takahashi [*]

Department of Physics and Information Technology, Kyushu Institute of Technology, Kawazu 680-4, Iizuka 820-8502, Japan; Research Institute for Information Technology, Kyushu University, 744 Motooka Nishi-ku, Fukuoka 819-0395, Japan; and AcsiomA Ltd, 3-8-33 Momochihama Sawara-ku, Fukuoka 814-0001, Japan

Kensuke S. Ikeda

Department of Physical Sciences, Ritsumeikan University, Noji-higashi 1-1-1, Kusatsu 525-8577, Japan

(Received 2 June 2023; revised 30 November 2023; accepted 6 March 2024; published 4 April 2024)

Sawtooth structures are observed in tunneling probabilities with changing Planck's constant for a periodically perturbed rounded-rectangular potential with a sufficiently wide width for which instanton tunneling is substantially prohibited. The sawtooth structure is a manifestation of the essential nature of multiquanta absorption tunneling. Namely, the periodic perturbation creates an energy ladder of harmonic channels at $E_n = E_I + n\hbar\omega$, where E_I is an incident energy and ω is an angular frequency of the perturbation. The harmonic channel that absorbs the minimum amount of quanta of $n = \bar{n}$, such that $V_0 < E_{\bar{n}} \leqslant V_0 + \hbar\omega$, makes a dominant contribution to the tunneling process, where V_0 is the height of the static potential and $V_0 - E_I \gg \hbar\omega$. At each steep slope part of the sawtooth structure, replacement of the dominant harmonic channel, i.e., $E_{\bar{n}} \to E_{\bar{n}+1}$, occurs and the tunneling probability suddenly drops with increasing $1/\hbar$. Due to the flatness of the potential top, resonance eigenstates exist just above the potential and the first resonance state appears as the peak of each edge of the sawtooth structure for the tunneling probability in the potential region. Sawtooth structures are also observed with changing the perturbation frequency. We introduce an effective formula to characterize the basic profile of those sawtooth structures.

DOI: 10.1103/PhysRevE.109.044203

I. INTRODUCTION

Tunneling observed for classically nonintegrable systems is essentially different from tunneling for classically integrable systems, which is mainly explained by the instanton theory [1–3]. In particular, tunneling that appears as a form of dynamical tunneling for quantum maps, periodically perturbed one-dimensional systems, and two-dimensional systems has attracted many authors' attention in the past three decades [1–4]. The tunneling process and its underlying mechanism change depending on the situation and several types of tunneling processes have been reported and theoretically studied from various viewpoints.

In the case that twin tori regions are embedded in a chaotic sea in the phase space, a so-called mixed system, the tunneling doublets of localized quasimodes corresponding to twin tori are no longer isolated in the spectrum and interact with states associated with the chaotic sea [5,6]. Indeed, the doublets are disturbed by a third level associated with the chaotic sea and the statistical nature of the fluctuations of the level splittings are theoretically explained by the prediction based on a random matrix model of the chaotic sea [6]. Then, the tunneling rate between twin tori is considerably enhanced compared with that for the classical integrable system. So it is called chaos-assisted tunneling (CAT). Evidence for CAT has been observed experimentally—for example, dynamical tunneling observed for microwave billiards and modulated optical lattice potentials [7].

For a nearly integrable system with twin tori, a visible chaotic region may be restricted to a dominant saddle and the phase space may be almost occupied by tori regions, which are symmetric with respect to the saddle, namely tunneling doublets exist in the spectrum regime. Even in this case, the tunneling rate between twin tori is considerably enhanced. This phenomenon has been theoretically explained by the notion of resonance-assisted tunneling (RAT) for the case that classically nonlinear resonances form non-negligible island chains in the classical phase space [8]. The theory of RAT provides an underlying picture that a tunneling path via a succession of classically forbidden transitions across nonlinear resonances is selected and considerably enhances the tunneling rate of twin tori when the (reduced) Planck constant $\hbar$ becomes relatively small.

The theory of RAT has been further improved and applied to a simpler case of dynamical tunneling from a regular region (tori) to a chaotic region [9–12]. In this case, several resonance peaks appear with changing $1/\hbar$ in the semiclassical regime. The theory of RAT gives a qualitative recipe identifying the relevance of nonlinear resonances: the tunneling path via one or multiple nonlinear resonances dominates the tunneling process and provides a quantitative prediction at a resonance peak. In this situation, the existence of resonance peaks associated with classical nonlinear resonances is the main reason for the enhancement of tunneling probability.

[*] takahasi@acsioma.jp

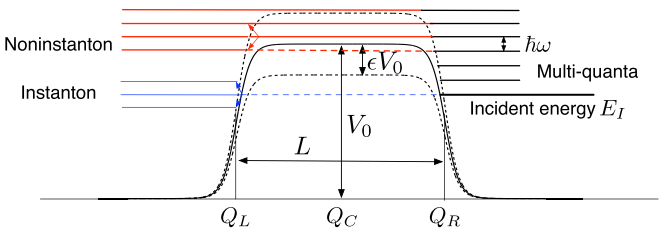

FIG. 1. Schematic picture of instanton tunneling and noninstanton tunneling (multiquanta absorption tunneling) for a periodically perturbed rounded-rectangular potential.

For the scattering problem of periodically perturbed barriers, an increase in tunneling probability owing to a mechanism different from CAT and RAT is observed [13–18]. As shown in Fig. 1, an energy ladder created by Floquet's theory induces a tunneling process, which is also different from instanton tunneling; for the instanton, see Refs. [19,20]. Namely, the transition from an input channel with energy $E = E_I$ to harmonic channels with energy $E = E_I + n\hbar\omega$ above the top of the potential barrier induces multiquanta absorption tunneling (MQAT), where ω is the angular frequency of the perturbation [18,21,22]. When these transition probabilities become larger than that of instanton, this tunneling process makes its appearance. In terms of semiclassics, this tunneling process is interpreted as the stable-unstable manifold guided tunneling (SUMGT); thus its mechanism is different from that of instanton-type tunneling [14–18,21,23]. The plateau spectrum observed for a scattering spectrum is a quantum mechanical manifestation of an unstable manifold [15,16].

This type of tunneling should apply to nearly integrable systems that have a single dominant saddle in the classical phase space so that in the integrable limit, the saddle works like an energetic barrier, the tunneling through which can be explained by the instanton theory. In this paper, we use the term "noninstanton" as a generic term for the tunneling which is observed for those nearly integrable systems and whose mechanism is not explained by the instanton theory [18,21]. This situation is suitable for studying the transition between tunneling for classically integrable systems, i.e., instanton tunneling, and that for classically nonintegrable systems, i.e., noninstanton tunneling [5,6,13–18,21,23–26].

Hanada *et al.* reported the enhancement of probabilities owing to this type of tunneling process for nearly integrable discrete-time systems with tiny island chains, i.e., the Hénon map, and the standard map [27–29]. The tunneling probability forms a staircase structure as a function of quantum numbers assigned to initial states. They argued that the successive switching among the harmonic channels with decreasing the quantum number is the key mechanism generating the staircase structure and this mechanism was called the resonant multiquanta excitation mechanism (RMEM) [28,29]. Namely, the movement of dominant harmonic channels from the outside of the separatrix to the inside induces a change from a flat part to a steep slope part of the staircase structure. Then, the subsequent replacement of dominant harmonic channels from inside ones to different ones outside causes a transition to the next flat part. When the energy of a quantized torus coincides with one of the dominant harmonic channels, the staircase structure is accompanied by a spike induced by such a quantized torus. Their result indicates that a staircase like structure as a function of a dynamical parameter, e.g., the Planck constant, generally appears for the tunneling process owning to MQAT.

In this paper, we explore and clarify the basic nature of staircase and sawtooth structures, which appear as a manifestation of noninstanton tunneling for discrete and continuous time systems with a single dominant saddle in the nearly integrable regime [28–31]. A periodically perturbed rounded-rectangular potential is suitable for this purpose for the following reasons. When the width of the potential is wide enough, instanton tunneling is substantially prohibited and the nature of noninstanton tunneling induced by a periodic perturbation is purely extracted [22]. Furthermore, plateau structures are observed for scattering spectra [22]. Our situation is out of the RAT regime in the sense that the system has no nonlinear resonances in the real classical phase space. On the other hand, there exist purely quantum resonance eigenstates above the potential top, which have no classical counterparts, namely no quantized real periodic orbits or tori [31]. Thus we investigate the influence of quantum resonance eigenstates on the tunneling process.

According to the previous works [18,21], the tunneling probability induced by the noninstanton tunneling decreases exponentially in the limits of $\omega \to 0$ and ∞. If instanton and noninstanton tunneling processes coexist, instanton tunneling governs in the limits of $\omega \to 0$ and ∞, but noninstanton tunneling, namely MQAT, takes relatively large values and can overwhelm instanton tunneling in a middle range. For the cases of periodically perturbed (rounded) step and (rounded) rectangular potentials with wide width [21–23], instanton tunneling is substantially prohibited and the noninstanton tunneling process is observed in the whole range of ω.

Under the above circumstance, we consider the problem of how the tunneling probability changes with either $1/\hbar$ or ω for a periodically perturbed rounded-rectangular potential with a wide width, in particular how the staircase or sawtooth structure is observed as a function of $1/\hbar$ or ω. We also pay attention to the problem of how the tunneling probability changes depending on the perturbation strength as a power law or exponential growth [22]. When the potential width is sufficiently wide, marked resonance eigenstates exist in the range $E > V_0$ [22]. Thus we consider the problem of how resonance eigenstates affect and enhance the tunneling process generated by MQAT.

This paper is organized as follows.

In Sec. II, we introduce a model system and explain the setup of quantum calculation. In Sec. III, we explain the properties of the wave function on an oscillating flat-top potential and the underlying mechanism of MQAT taking a periodically perturbed step potential as a simple example. We also mention the relationship among MQAT, RAT, and CAT. In Sec. IV, we show numerical results. Namely, tunneling probabilities in the potential and transmissive regions change like a sawtooth function with either $1/\hbar$ or ω. In particular, the sawtooth structure of the potential region is accompanied by resonance peaks due to the effect of resonance eigenstates. In Sec. V, we consider the basic profile of the sawtooth structure by introducing an effective formula relying on the results

of the previous works [18,21]. Section VI is devoted to a discussion.

II. MODEL AND QUANTUM WAVE OPERATOR

The system studied in this paper is a periodically perturbed rounded-rectangular potential given by [22]

$$\hat{H}(Q,P,\omega t)=\frac{1}{2M}P^2+(1+\epsilon\,\sin\omega t)V_{R0}(Q), \tag{1}$$

where $V_{R0}(Q)$ is the unperturbed potential set as

$$V_{R0}(Q)=\{1+\exp[-(Q-Q_L)]\}^{-1}-\{1+\exp[-(Q-Q_R)]\}^{-1}. \tag{2}$$

All the dynamical values and parameters are dimensionless. We set the mass as $M=1$. The width and center of the potential barrier are given by $L\equiv Q_R-Q_L$ and $Q_C\equiv(Q_R+Q_L)/2$, respectively, and the height of the unperturbed potential is defined as $V_0\equiv V_{R0}(Q_C)$ (see Fig. 1). We set $L=30$, thus $1-V_0\sim 6.118\times10^{-7}$, and set the right edge of the potential barrier at $Q_R=0$ throughout this paper. In the limit of $Q_L\to-\infty$, the rounded-rectangular potential $V_{R0}(Q)$ converges to a rounded-step potential [21,23].

We consider the case that a plane wave is injected from positive infinity in Q with a constant momentum $P_I(<0)$, where the subscript of dynamical variables, "I," indicates input. Thus a scattering eigenstate, more precisely a quasi-stationary state, is represented by the wave operator [13,32],

$$\langle Q|\hat{\Omega}_1^+(t)|P_I\rangle=\lim_{|Q_I|\to\infty}\sqrt{\frac{|P_I|}{2\pi\hbar M}}e^{iP_IQ_I/\hbar}\int_0^\infty ds\times\langle Q|\hat{U}(\omega t:\omega t-\omega s)|Q_I\rangle\exp\left\{\frac{i}{\hbar}E_Is\right\}, \tag{3}$$

where initial energy is given by $E_I=P_I^2/2M$ and $\hat{U}$ denotes the propagator of the system,

$$\hat{U}(\theta+\omega t:\theta)=\mathcal{T}\exp\left\{-\frac{i}{\hbar}\int_0^t\hat{H}(\theta+\omega s)ds\right\}, \tag{4}$$

where $\mathcal{T}$ indicates the time ordering operator.

For the case of a free particle with $V_{R0}=0$, the wave operator (3) provides a plane wave as

$$\langle Q|\hat{\Omega}_1^+(t)|P_I\rangle|_{V_{R0}=0}=\frac{1}{\sqrt{2\pi\hbar}}e^{\frac{i}{\hbar}(P_IQ-E_It)}. \tag{5}$$

To kill the dependence in amplitude on $\hbar$ for convenience in the following study, we renormalize the momentum eigenstate as

$$|\bar{P}_I\rangle\equiv\sqrt{2\pi\hbar}|P_I\rangle. \tag{6}$$

Then, the scattering eigenstate is given as

$$\langle Q|\hat{\Omega}_1^+(t)|\bar{P}_I\rangle=\lim_{|Q_I|\to\infty}\sqrt{\frac{|P_I|}{M}}e^{iP_IQ_I/\hbar}\int_0^\infty ds\times\langle Q|\hat{U}(\omega t:\omega t-\omega s)|Q_I\rangle\exp\left\{\frac{i}{\hbar}E_Is\right\}. \tag{7}$$

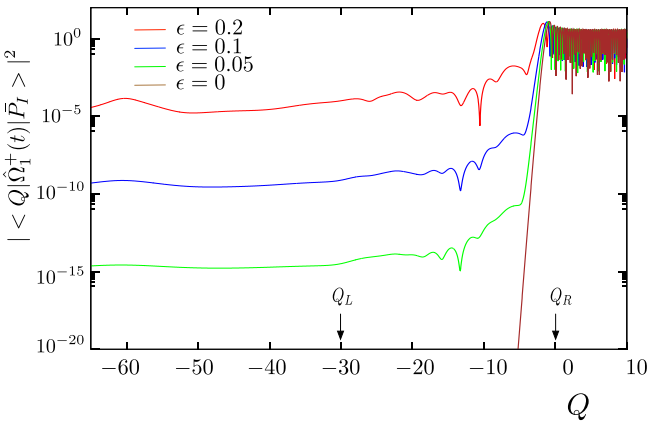

FIG. 2. Probability densities of scattering eigenstates $|\langle Q|\hat{\Omega}_1^+(t=0)|\bar{P}_I\rangle|^2$ at $\epsilon=0.0$, 0.05, 0.1, and 0.2 with $E_I=0.75$, $\omega=0.3$, and $\hbar=\hbar_{\rm ref}=1000/(3\pi\times2^{10})\sim0.1036165$.

We show scattering eigenstates at an off-resonance condition taking Planck's constant as $\hbar=\hbar_{\rm ref}\equiv1000/(3\pi\times2^{10})\sim0.1036165$, which are very similar to those for the case of $L=20$ studied in the previous work [22]. Hereafter, we take this value of $\hbar_{\rm ref}$ as the reference value of Planck's constant. Scattering eigenstates are calculated by using the symplectic integrator including a plane wave generator [32]. Note that resonance eigenstates for the condition of $E_I>V_0$ are shown in Appendix A.

Figure 2 shows probability densities at $t=0\,(\mathrm{mod}\,T)$ with $T=2\pi/\omega$ for four representative values of ϵ, $\epsilon=0$, 0.05, 0.1, and 0.2, where the remaining parameters are taken as $E_I=0.75$ and $\omega=0.3$. For the unperturbed system with $\epsilon=0$, the tunneling tail penetrating into the potential barrier can be explained by instanton tunneling and drops off exponentially. For the perturbed system, the tunneling probability is enhanced due to MQAT and increases with ϵ. For each scattering eigenstate, the probability density takes larger values near the right edge of the potential, while it takes almost constant values accompanied by a small undulation in the left half of the potential region $Q_L<Q<Q_C$. The probability density in the range $Q<Q_L$ takes values slightly less than those in the potential region and gradually undulates due to the periodic perturbation.

To evaluate tunneling probabilities in the potential and transmissive regions, we introduce the following quantities, P_p^Q and P_t^Q:

$$P_p^Q\equiv\frac{2}{L}\int_{Q_L}^{Q_C}|\langle Q|\hat{\Omega}_1^+(t=0)|\bar{P}_I\rangle|^2dQ, \tag{8}$$

$$P_t^Q\equiv\frac{1}{Q_{te}-Q_{ts}}\int_{Q_{ts}}^{Q_{te}}|\langle Q|\hat{\Omega}_1^+(t=0)|\bar{P}_I\rangle|^2dQ, \tag{9}$$

where Q_{te} and Q_{ts} are set as $Q_{te}=Q_L-5.0$ and $Q_{ts}=Q_{te}-T\sqrt{2V_0/M}$, respectively. Namely, P_p^Q provides mean probability density over the left half of the potential region to avoid large irregular oscillations near the right end and P_t^Q gives the amplitude averaged over a nearly spatial period in the transmissive region, which roughly corresponds to a time average of the tunneling probability through the potential.

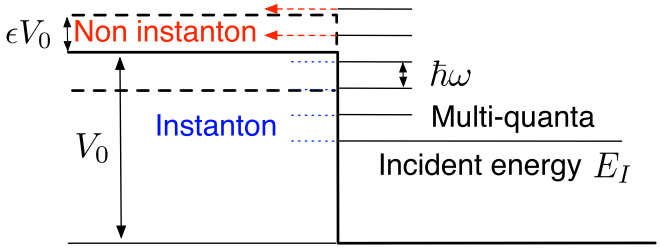

FIG. 3. Schematic picture of multiquanta absorption tunneling for a periodically perturbed step potential.

III. WAVE PROPERTIES ON THE OSCILLATING FLAT TOP FOR A PERIODICALLY PERTURBED STEP POTENTIAL AND MQAT

Before going to numerical analysis, let us consider the properties of the wave function in the potential region taking a periodically perturbed step potential studied in the previous work as a simplified example [21]. Owing to the periodic perturbation, harmonic channels are generated by multiquanta absorption and emission forming an energy ladder, $E_n = E_I + n\hbar\omega$. Figure 3 schematically shows the multiquanta absorption tunneling (MQAT) for the periodically perturbed step potential. Note that sawtooth structures are also observed for this case, although we do not show results [30].

On the other hand, the oscillation of the flat-top potential, $V(t) = V_0(1 + \epsilon \sin\omega t)$, adds a time-dependent phase modulation to a wave function in the potential region as [33]

$$\Psi(Q,t) = \exp\left(i\frac{\epsilon V_0}{\hbar\omega}\cos\omega t\right)\Psi_0(Q,t), \tag{10}$$

where $\Psi_0(Q,t)$ is a wave function in the potential region for the unperturbed system. Thus, for the periodically perturbed systems, a scattering eigenstate with incident energy E_I is represented in the potential region as

$$\Psi(Q,t) = \sum_n C_n\Psi_n(Q,t), \tag{11}$$

where C_n are constants of complex values and each $\Psi_n(Q,t)$ denotes a modulated harmonic channel at $E = E_n$ given by

$$\Psi_n(Q,t) = \exp\left[\frac{i}{\hbar}\left(\frac{\epsilon V_0}{\omega}\cos\omega t - E_n t\right)\right]\Psi_{0,n}(Q), \tag{12}$$

where $\Psi_{0,n}(Q)$ is the scattering eigenstate of the unperturbed system at $E = E_n$. Hereafter, we simply call the modulated harmonic channel by the harmonic channel. In the case of the step potential, $\Psi_{0,n}(Q)$ with energy $E_n > V_0$ is regarded as a plane wave with the momentum of a nonzero real value in the potential region. In contrast, for $E_n < V_0$, the momentum takes an imaginary value like instanton. Thus harmonic channels with $E_n < V_0$ do not substantially contribute, while harmonic channels with $E_n > V_0$ contribute to MQAT.

Since the probabilistic weight of each harmonic channel is given by $|C_n\Psi_n(Q,t)|^2$, the transition rate from the incident plane wave with $E = E_I$ to each harmonic channel with $E_n > V_0$, i.e., $P_{\rm tr}(n) = |C_n|^2$, is the key to evaluating the contribution of the harmonic channel to MQAT. Figure 4 schematically shows $P_{\rm tr}(n)$ as a function of the order of the harmonic channel n, where an approximate formula for $P_{\rm tr}(n)$ given in Sec. V is used in advance [21]. In the range $0 \leqslant n \lesssim \frac{e\epsilon V_0}{2\hbar\omega}$, which corresponds to the classically accessible energy range caused by the periodic perturbation, $P_{\rm tr}(n)$ takes values of the same order; thus it is approximately represented by a constant function. In the range $n \gtrsim \frac{e\epsilon V_0}{2\hbar\omega}$, namely the tunneling regime, $P_{\rm tr}(n)$ decreases more than exponential functions with n. Thus the harmonic channel with the energy such that $V_0 < E_n \leqslant V_0 + \hbar\omega$ dominantly contributes to MQAT when instanton tunneling is prohibited.

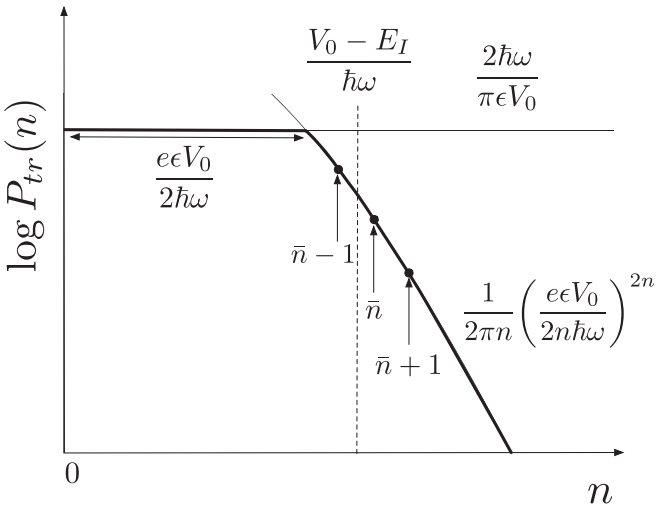

FIG. 4. Schematic picture of the transition rates $P_{\rm tr}(n)$ from the incident plane wave to harmonic channels.

The above argument should apply to the periodically perturbed rounded-rectangular potential with a wide width, since it has an almost flat top and instanton tunneling is substantially prohibited (see Fig. 1). Then, the order of the dominant harmonic channel $\bar{n}$ is specified as

$$\bar{n} = \min\{n | n\hbar\omega > V_0 - E_I, n \in \mathbf{N}\} \tag{13}$$

and $E_{\bar{n}}$ is given as

$$E_{\bar{n}} = E_I + \bar{n}\hbar\omega. \tag{14}$$

Thus there is a critical condition that one of the harmonic channels satisfies the condition $E_n = V_0$. When either Planck's constant $\hbar$ or angular frequency ω is taken as a control parameter, the critical condition for a given n is satisfied at $\hbar = \hbar_n^c$ or $\omega = \omega_n^c$, where $\hbar_n^c$ and ω_n^c are respectively defined as

$$\hbar_n^c \equiv \frac{V_0 - E_I}{n\omega}, \tag{15}$$

$$\omega_n^c \equiv \frac{V_0 - E_I}{n\hbar}. \tag{16}$$

Let us call $\hbar_n^c$ and ω_n^c the switching points in the following sense. From the above discussion, when $\hbar$ passes through each switching point $\hbar_n^c$, a sudden change of tunneling probability should be observed. In a neighborhood of each $\hbar_n^c$, the dominant harmonic channel is given by $\bar{n} = n$ for $\hbar > \hbar_n^c$ and by $\bar{n} = n + 1$ for $\hbar < \hbar_n^c$; thus the tunneling probability abruptly decreases when $\hbar$ decreases and passes through $\hbar_n^c$. The same is true in the case that ω passes through ω_n^c. This means that the tunneling probability forms a sawtooth structure as a function of $1/\hbar$ or ω. For the case of $\omega > \omega_1^c$,

the single-quantum absorption tunneling (SQAT) dominates the tunneling process and the tunneling probability should be decreased almost exponentially with increasing ω like in the case of a periodically perturbed rounded-step potential [21].

As shown in the previous work [22], the periodically perturbed rounded-rectangular potential has resonance eigenstates, each of which has a complex eigenenergy E_m^r ($\mathrm{Re}E_m^r > V_0$) accompanied by harmonic channels (see Appendix A). When the synchronization with the dominant harmonic channel, i.e., $\mathrm{Re}E_m^r = E_{\bar{n}}$, occurs for a lower-order resonance state, e.g., $m = 1$ or 2, this should affect the tunneling process and enhance a tunneling probability in the potential region. This point should be confirmed with numerical simulation.

In the above discussion, we assume that the transition rate $P_{\mathrm{tr}}(n)$ among the harmonic channels is a fairly regular function of n and the resonance eigenstates and their eigenenergies under perturbation are close to those of the unperturbed system. Let us consider the applicability of the above scenario to tunneling processes for nearly integrable systems. For periodically perturbed systems, energy levels except continuous spectrum are written owing to Floquet's theory as the following set:

$$E_{\mathrm{lev}} = \{E_{m,n} | E_{m,n} = E_m + n\hbar\omega\}, \tag{17}$$

where $\{E_m\}$ denote input energy and energy eigenvalues close to those of an integrable system and $\{E_{m,n}\}$ for each m denote harmonic channels of E_m.

For scattering potentials without resonance states, e.g., the Eckart barrier, we can take E_0 as input energy, namely $E_0 = E_I$, and the others are removed. Thus there exists a single energy ladder $E_{0,n} = E_0 + n\hbar\omega$. If the potential width is sufficiently large, namely the contribution of instanton is sufficiently small, a sawtooth structure should be observed. For scattering potentials with resonance states as in the present case, we also take $E_0 = E_I$ and assign E_m ($m > 0$) for resonance energies as $E_m = E_m^r$. For a potential with a wide width, a sawtooth structure should be observed and the resonance condition $\mathrm{Re}\, E_m^r - E_0 = n\hbar\omega$ should cause an additional effect on the tunneling process.

For nearly integrable quantum maps with a dominant saddle and without (visible) nonlinear resonances, the energy level set, $\{E_m\}$, in Eq. (17) can be taken to be close to that of the unperturbed system. From the observations of tunneling behavior [27–29], the underlying mechanism of the tunneling process should be similar to that mentioned above.

For nearly integrable quantum maps involving visible nonlinear resonance(s), namely in the RAT regime [8–12], at least a part of energy levels corresponding to the nonlinear resonance(s) and their eigenfunctions are fairly deformed from unperturbed ones. In this case, the transition probabilities among the harmonic channels for each E_m via nonlinear resonance(s) should fairly deviate from those for systems without (visible) nonlinear resonances, but the resonance condition $\mathrm{Re}\, E_m^r - E_0 = n\hbar\omega$ should still play an important role. Thus the underlying mechanism of the tunneling process via nonlinear resonance(s) should be fairly modified and either an additional scenario or another different scenario, e.g., the RAT theory, should be needed to explain the tunneling process [8–12].

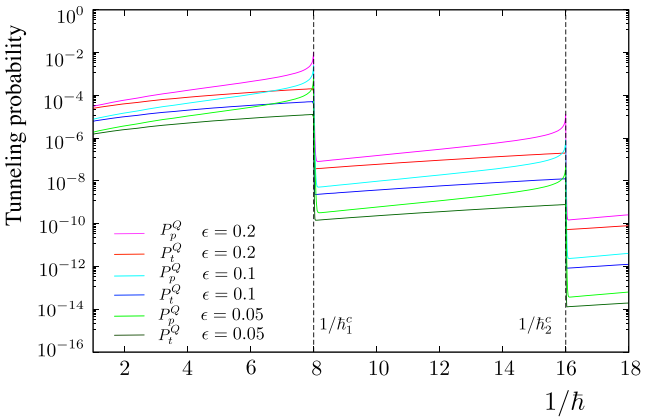

FIG. 5. Changes of tunneling probabilities P_p^Q and P_t^Q as functions of $1/\hbar$ with $\omega = 2.0$ and $E_I = 0.75$ for $\epsilon = 0.05$, 0.1, and 0.2. Broken vertical lines denote $1/\hbar_1^c$ and $1/\hbar_2^c$.

For quantum maps with mixed phase space, namely in the CAT regime [5,6], most energy levels are significantly different from those of the unperturbed system and their eigenfunctions are largely deformed from unperturbed ones. For this case, the underlying mechanism of the tunneling process should be completely different from that mentioned above and detail processes should sensitively depend on the situation, e.g., the detail of the classical phase structure.

IV. CHANGE OF TUNNELING PROBABILITIES WITH $\hbar$ AND ω

A. Change of tunneling probabilities with $\hbar$

In this subsection, we consider how the tunneling probabilities in the potential and transmissive regions change with Planck's constant $\hbar$.

1. Change of tunneling probabilities at $\omega = 2.0$

First, we consider the case of $\omega = 2.0$, where one or a few quanta majorly contribute to the tunneling process. Figure 5 shows P_p^Q and P_t^Q as functions of $1/\hbar$ for the cases of $\epsilon = 0.05$, 0.1, and 0.2, which form sawtooth structures, and P_p^Q is always larger than P_t^Q at each value of ϵ. Actually, very sharp transitions of P_p^Q and P_t^Q are observed near the switching points $1/\hbar_1^c \sim 8$ and $1/\hbar_2^c \sim 16$ owing to the replacement of the dominant harmonic channel. The single-quantum absorption tunneling with $\bar{n} = 1$ is dominant in the region $1/\hbar < 1/\hbar_1^c$, the two-quanta absorption tunneling with $\bar{n} = 2$ becomes dominant in the region $1/\hbar_1^c \leqslant 1/\hbar < 1/\hbar_2^c$, and so on. Furthermore, P_p^Q have sharp peaks corresponding to the first resonance state at $E_{\bar{n}} \sim \mathrm{Re}E_1^r$, each of which appears just before the switching point. In each of the regions, $1/\hbar < 1/\hbar_1^c$ and $1/\hbar_1^c \leqslant 1/\hbar < 1/\hbar_2^c$, P_t^Q increase slightly less than exponential functions with $1/\hbar$, while P_p^Q grow more than exponential functions due to the wide skirts of the resonance peaks. Values of P_p^Q and P_t^Q increase with increasing ϵ when $\hbar$ is fixed. From the comparison of the cases of $\epsilon = 0.05$, 0.1, and 0.2, the increasing rates of P_p^Q and P_t^Q with ϵ are not markedly changed with $1/\hbar$ as long as $\bar{n}$ takes the same value,

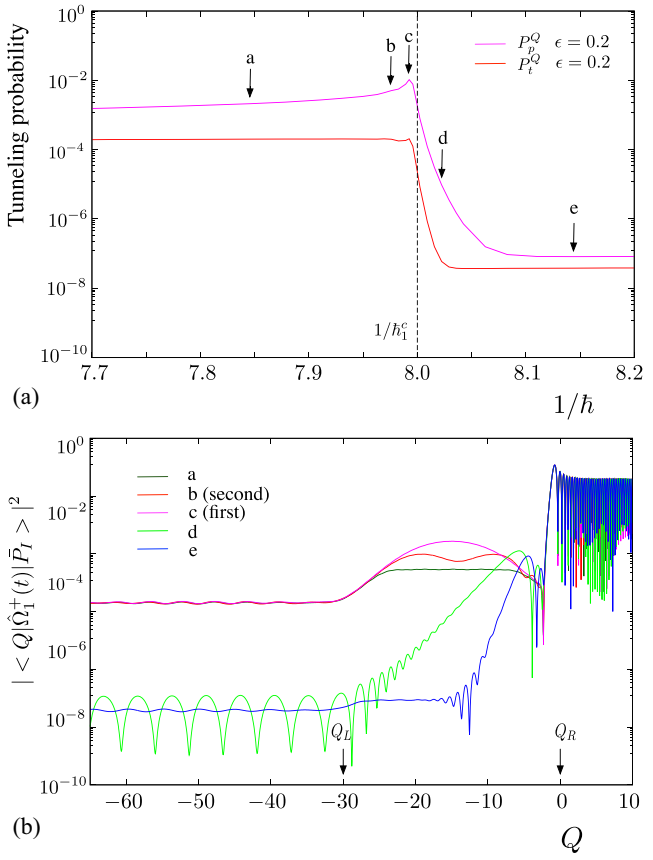

FIG. 6. Tunneling probabilities and probability densities at $\epsilon = 0.2$ near the first switching point $1/\hbar_1^c$ in Fig. 5. (a) Changes of tunneling probabilities P_p^Q and P_t^Q as functions of $1/\hbar$. The labels from "a" to "e" denote representative values of $\hbar$ in Table I. (b) Probability densities $|\langle Q|\hat{\Omega}_1^+(t=0)|\bar{P}_I\rangle|^2$ at the representative values of $\hbar$.

but clearly change when $\bar{n}$ is replaced, e.g., the rates at $\bar{n} = 2$ are apparently larger than those at $\bar{n} = 1$.

Figure 6(a) shows the variations of P_p^Q and P_t^Q in a neighborhood of $1/\hbar_1^c$ at $\epsilon = 0.2$ and 6(b) shows probability densities at representative values of $\hbar$ labeled from "a" to "e" in 6(a) (also see Table I). For the case of "c," at which the peak of the first resonance state appears in Fig. 6(a), a single hump is observed in the potential region in Fig. 6(b). This means that the first resonance state is excited owing to the synchronization with the dominant harmonic channel, namely the first harmonic channel in this case, under the condition $\mathrm{Re}E_1^r = E_{\bar{n}}$, and majorly forms probability density in the potential region. Actually, the contributions of harmonic channels with $n > \bar{n}$ are negligible because their transition rates $P_{\mathrm{tr}}(n)$ are exponentially smaller than that of the dominant harmonic channel and further no lower-order resonance states with E_m^r $(m > 1)$ synchronize with the $(\bar{n}+1)$th harmonica channel because $\mathrm{Re}E_m^r \ll E_{\bar{n}+1}$ when ω is sufficiently large.

For the case of "b," which corresponds to the second resonance state, twin peaks are observed in the potential region in Fig. 6(b), although no clear resonance peak is observed in Fig. 6(a) because the wide skirt of the first resonance peak hides it. For the case of "a" in the off-resonance condition, it forms a tablelandlike distribution in the potential region. In the transmissive region, the probability densities for the cases of "a," "b," and "c" form almost flat distributions taking nearly the same values but accompanied by small undulation. This means that the resonance eigenstates do not influence the probability density in the transmissive region. However, this fact does not contradict the fact that the resonance eigenstates have long lifetimes and rather allows them to do so because of relatively smaller leak rates.

For the case of "d" in the transition region around the switching point $1/\hbar_1^c$, as shown in Fig. 6(b), it exponentially decreases being accompanied by a high-frequency oscillation with gradually increasing amplitude as Q decreases in the potential region, while it periodically oscillates with large amplitude in the transmissive region. For the case of "e," namely, just after the transition, as Q decreases, it rapidly decays being accompanied by a gradually increasing high-frequency oscillation in the right half of the potential region, while it forms a nearly flat distribution in the left half. Then, it takes an almost flat distribution with small undulation in the transmissive region. Therefore, the probability densities of "d" and "e" take smaller values in the transmissive region than those of "a," "b," and "c" owing to the replacement of the dominant harmonic channel, but that of "d" oscillates with large amplitude because it is in the critical condition.

TABLE I. Representative values of Planck's constant $\hbar$.

	ω	$\hbar/\hbar_{\mathrm{ref}}$	$\hbar$	$1/\hbar$
a	2.0	1.23	0.1274483	7.84631921
b (2nd)	2.0	1.21	0.1253769	7.97601043
c (1st)	2.0	1.2075	0.1251169	7.99252391
d	2.0	1.203	0.1246506	8.02242113
e	2.0	1.185	0.1227856	8.14428070
f	0.3	9.5	0.9843567	1.0158918
g (2nd)	0.3	8.6	0.8911019	1.1222061
h (1st)	0.3	8.2	0.8496553	1.1769479
i	0.3	8.0	0.8289320	1.2063716
j	0.3	6.7	0.6942305	1.4404437
k	0.3	1.02	0.1056888	9.46173787
l (2nd)	0.3	1.008	0.1044454	9.57437761
m (1st)	0.3	1.006	0.1042382	9.59341216
n	0.3	1.005	0.1041346	9.60295784
o	0.3	1.0	0.1036165	9.65097263

2. *Change of tunneling probabilities at* $\omega = 0.3$

Here, we consider the case of $\omega = 0.3$ in the MQAT regime. Figure 7 shows P_p^Q and P_t^Q as functions of $1/\hbar$ for the cases of $\epsilon = 0.05$, 0.1, and 0.2. At each value of ϵ, P_p^Q and P_t^Q form sawtooth structures and P_p^Q is always larger than P_t^Q. Indeed, abrupt changes of P_p^Q and P_t^Q are observed near every switching point $1/\hbar_n^c$ given by Eq. (15) and P_p^Q have clear resonance peaks, each of which appears just before $1/\hbar_n^c$. An average line (or baseline) of P_p^Q or P_t^Q, which is, for example, defined as a mean line of the upper and lower envelope lines of the sawtooth structure in a logarithmic scale,

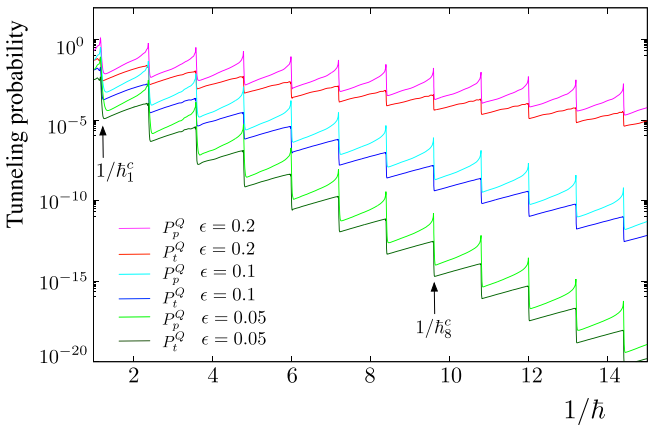

FIG. 7. Changes of tunneling probabilities P_p^Q and P_t^Q as functions of $1/\hbar$ at $\omega = 0.3$ and $E_I = 0.75$ for $\epsilon = 0.05$, 0.1, and 0.2.

decreases exponentially with $1/\hbar$ as $\propto \exp[-C(\epsilon)/\hbar]$, where $C(\epsilon)$ decreases with increasing ϵ. In every interval between the nearest switching points, $1/\hbar_n^c$ and $1/\hbar_{n+1}^c$, P_t^Q increases with $1/\hbar$ slightly less than exponential functions, while P_p^Q grows more than exponential functions due to the wide skirt of the resonance peak.

Figure 8(a) shows the variations of P_p^Q and P_t^Q in a neighborhood of $1/\hbar_1^c$ at $\epsilon = 0.2$ and 8(b) shows probability densities at representative values of $\hbar$ labeled from "f" to "j" in 8(a) (also see Table I). Figure 9(a) shows P_p^Q and P_t^Q in a neighborhood of $1/\hbar_8^c$ and 9(b) shows probability densities at representative values of $\hbar$ labeled from "k" to "o" in 9(a) (also see Table I). Since "o" is the case of $\hbar_{\rm ref}$, the probability density labeled "o" in Fig. 9(b) is the same as that at $\epsilon = 0.2$ in Fig. 2.

As shown in Figs. 8(a) and 9(a), P_p^Q and P_t^Q suddenly fall off near $1/\hbar_n^c$ owing to the replacement of the dominant harmonic channel; P_p^Q and P_t^Q are steeper near $1/\hbar_8^c$ than near $1/\hbar_1^c$. At the values of $1/\hbar$ labeled "h" and "m," P_p^Q forms clear peaks corresponding to the first resonance states, while P_t^Q takes local maximum values, which are not so large. Thus the synchronization between the dominant harmonic channel and the first resonance state does not significantly enhance the tunneling probability in the transmissive region, especially in the semiclassical regime, $\hbar\omega \ll 1$. As shown in Fig. 8(b) the probability density labeled "h" with $\bar{n} = 1$ has a single hump in the potential region, while in Fig. 9(b), the probability density labeled "m" with $\bar{n} = 8$ has a hump deformed by the harmonic channel of $n = \bar{n} + 1 = 9$, i.e., $E_{\bar{n}+1} = E_I + 9\hbar\omega$. Thus the subdominant harmonic channel of $n = \bar{n} + 1$ is not negligible and contributes to probability density in the potential region when $\hbar\omega$ is sufficiently small in the semiclassical regime.

The probability densities labeled "g" and "l" should correspond to the second resonance states. In Figs. 8(a) and 9(a), they individually make small bumps on the skirts of the first resonance peaks. In Fig. 8(b), the probability density labeled "g" takes smaller values near the center and larger values near the left and right ends in the potential region, while in Fig. 9(b), the probability density labeled "l" forms twin peaks deformed by the subdominant harmonic

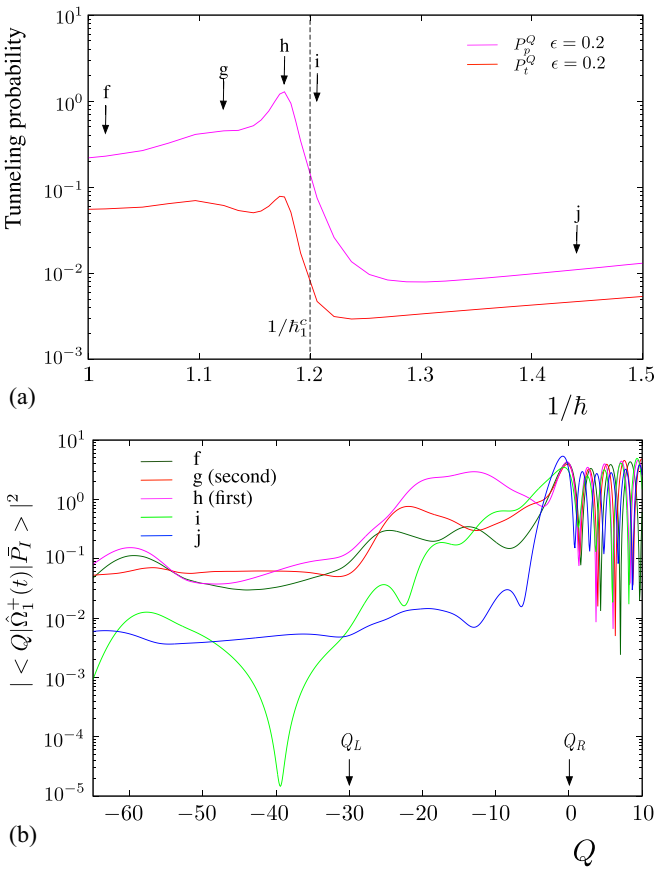

FIG. 8. Tunneling probabilities and probability densities at $\epsilon = 0.2$ near the first switching point $1/\hbar_1^c$ in Fig. 7. (a) Changes of tunneling probabilities P_p^Q and P_t^Q as functions of $1/\hbar$. The labels from "f" to "j" denote representative values of $\hbar$ in Table I. (b) Probability densities at the representative values of $\hbar$.

channel of $n = \bar{n} + 1$. The states labeled "f" and "k" are out of resonance but their probability densities take relatively large values in the potential region: it undulates in Fig. 8(b) and it behaves as a higher resonance mode in Fig. 9(b).

In Figs. 8(a) and 9(a), the states labeled "i" and "n" are in the steep transition regions and very close to $1/\hbar_1^c$ and $1/\hbar_8^c$, respectively. As shown in Figs. 8(b) and 9(b), they almost exponentially decrease being accompanied by high-frequency oscillations as Q decreases in the potential regions and have dips near $Q = -40$ in the transmissive region; in particular, that of "i" forms a deep valley. Thus these probability densities are more irregular than the others because they are in critical conditions at each of which the replacement of the dominant harmonic channel occurs. As shown in Figs. 8(a) and 9(a), the states labeled "j" and "o" are to the right of the transition regions. In Figs. 8(b) and 9(b), the probability densities of "j" and "o" rapidly decay with decreasing Q in the right half of the potential region, while in the left half nearly flat distributions accompanied by undulations are observed. Each of the probability densities of "j" and "o" takes smaller values in the transmissive region than those of the states on the left sides of the transition region because of the replacement of the dominant harmonic channel.

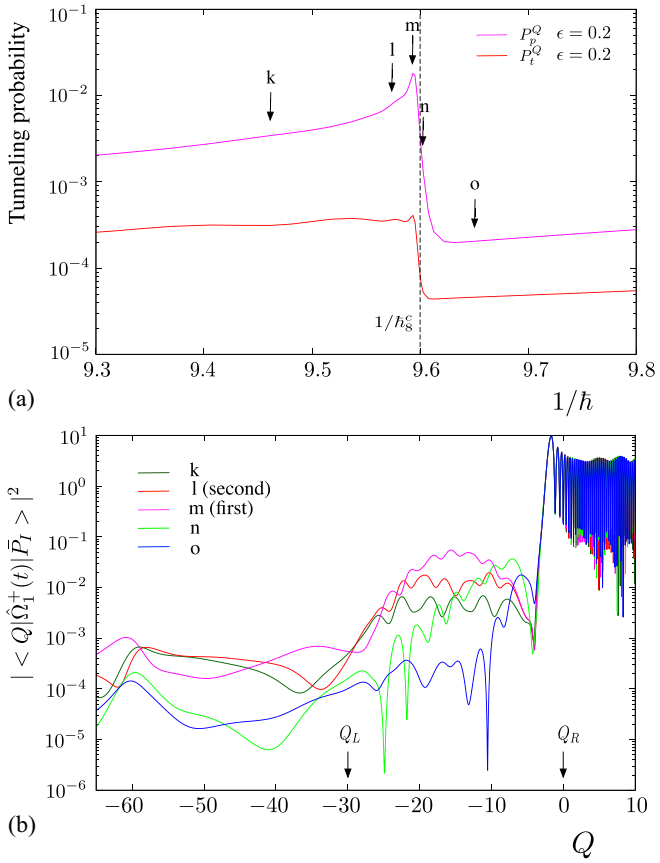

FIG. 9. Tunneling probabilities and probability densities at $\epsilon = 0.2$ near the eighth switching point $1/\hbar_8^c$ in Fig. 7. (a) Changes of tunneling probabilities P_p^Q and P_t^Q as functions of $1/\hbar$. The labels from "k" to "o" denote representative values of $\hbar$ in Table I. (b) Probability densities at the representative values of $\hbar$.

B. Change of tunneling probabilities with ω

In this subsection, we consider how the tunneling probabilities P_p^Q and P_t^Q change with ω at $\hbar = \hbar_{\rm ref}$. Figure 10 shows P_p^Q and P_t^Q as functions of ω for the cases of $\epsilon = 0.05$, 0.1, and 0.2. The tunneling probabilities P_p^Q and P_t^Q form sawtooth structures and the stepwise transitions occur at $\omega = \omega_n^c$ defined by Eq. (16), and P_p^Q have clear resonance peaks, each of which appears just after ω_n^c.

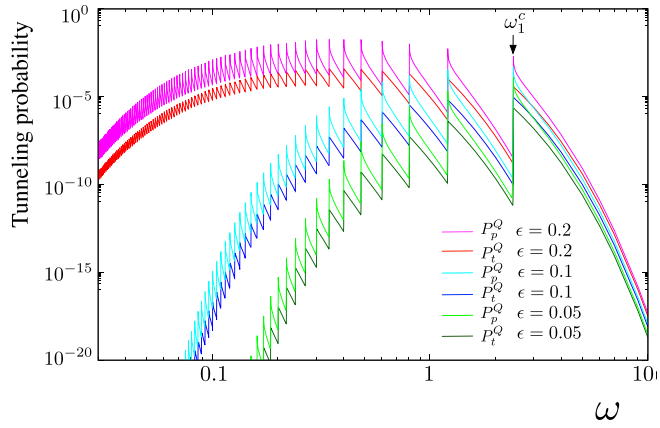

FIG. 10. Changes of tunneling probabilities P_p^Q and P_t^Q as functions of ω with $\hbar = \hbar_{\rm ref}$ and $E_I = 0.75$ for $\epsilon = 0.05$, 0.1, and 0.2.

In the region $\omega > \omega_1^c$, the single-quantum absorption tunneling (SQAT) governs the tunneling process and the tunneling probabilities decrease almost exponentially with ω, because the energy gap between the dominant harmonic channel of $\bar{n} = 1$ and the potential height V_0, i.e., $E_1 - V_0 = E_I + \hbar\omega - V_0$, increases with ω. Thus the quantum perturbation method based on the single-quantum absorption process should be available if an unperturbed solution is given analytically and the tunneling amplitude should be proportional to ϵ like that for the rounded-step potential in the previous work [21].

From Eq. (16), ω_n^c decreases as $\propto 1/n$ and the interval between the nearest switching points, i.e., $(\omega_{n+1}^c, \omega_n^c)$, decreases as $\propto 1/n(n+1)$ with increasing n. Thus switching points become densely in a low-frequency range. In each interval $(\omega_{n+1}^c, \omega_n^c)$, P_t^Q almost obeys a power-law decay $\propto \omega^{-\alpha_\omega}$ when $\bar{n}$ is sufficiently large and the absolute value of the exponent α_ω increases with $\bar{n}$. On the other hand, P_p^Q decreases faster than exponential functions of $1/\omega$ near the resonance peak but seems to obey a power-law decay far from the peak. Thus the tunneling probabilities P_p^Q and P_t^Q sensitively change with ω in a low-frequency range.

Average lines of P_p^Q and P_t^Q for $\omega < \omega_1^c$ take the maximum values in a middle range for $\epsilon = 0.2$, while they increase with ω except in neighborhoods of ω_1^c for $\epsilon = 0.1$ and 0.05. Thus the average lines almost exponentially decrease with decreasing ω in a low-frequency range. On the other hand, the average lines of P_p^Q (or P_t^Q) with $\epsilon = 0.05$, 0.1, and 0.2 approach each other when ω approaches ω_1^c and take values of the same order near $\omega = \omega_1^c$. Thus the growth rate of the mean tunneling probabilities with ϵ decreases as ω increases.

From the discussion so far, it is important to clarify the feature of the sawtooth structure as a function of $1/\hbar$ and ω. In the following section, we explore this issue.

V. BASIC PROFILE OF THE SAWTOOTH STRUCTURE

In this section, we consider the basic profile of the sawtooth structure as a function of $1/\hbar$ or ω relying on a formula introduced for periodically perturbed step and rectangular potentials in the previous works [18,21]. Namely, under a plausible assumption we introduced an approximate formula to evaluate the elements of the transition matrix, which gives the transition rate from the incident plane wave to one of the harmonic channels and we provided with the help of this formula a theoretical explanation for the generation mechanism of plateau spectra in the S matrix, which are commonly observed for periodically perturbed (rounded) step and barrier potentials. Based on the discussion in Sec. III, we assume that essentially the same formula is applicable for the rounded-rectangular potential and bring out the basic profile of the sawtooth structure relying on it.

According to the previous works [18,21], in the regime of $\hbar\omega \ll \epsilon$, the transition rate $P_{\rm tr}(n)$ from the incident plane wave with $E = E_I$ to a harmonic channel with $E_n = E_I + n\hbar\omega$ is

approximated by the Bessel function J_n as

$$P_{\rm tr}(n) \sim \left|J_n\left(\frac{\epsilon V_0}{\hbar\omega}\right)\right|^2 \sim \begin{cases} \frac{2\hbar\omega}{\pi\epsilon V_0} & \left(|n| \lesssim \frac{e\epsilon V_0}{2\hbar\omega}\right), \\ \frac{1}{2\pi n}\left(\frac{e\epsilon V_0}{2n\hbar\omega}\right)^{2n} & \left(|n| \gtrsim \frac{e\epsilon V_0}{2\hbar\omega}\right), \end{cases} \tag{18}$$

where we apply the asymptotic form of J_n for $n \gg 1$ to the range of $|n| \gtrsim \frac{e\epsilon V_0}{2\hbar\omega}$ [34]. As mentioned in Sec. III, the range $0 \leqslant n \lesssim \frac{e\epsilon V_0}{2\hbar\omega}$ corresponds to the classically accessible range owing to the perturbation and the range $n \gtrsim \frac{e\epsilon V_0}{2\hbar\omega} \sim \frac{\epsilon V_0}{\hbar\omega}$ corresponds to the tunneling regime induced by MQAT. Thus we focus on the latter range and rewrite $P_{\rm tr}$ as a function of E_n:

$$\begin{aligned} P_{\rm tr}(E_n, E_I) &\sim \frac{1}{2\pi n}\exp\left\{-2n\left[\ln\left(\frac{2n\hbar\omega}{\epsilon V_0}\right) - 1\right]\right\} \\ &= \frac{\hbar\omega}{2\pi(E_n - E_I)} \\ &\quad \times \exp\left\{-2\frac{E_n - E_I}{\hbar\omega}\left[\ln\left(\frac{2(E_n - E_I)}{\epsilon V_0}\right) - 1\right]\right\}. \end{aligned} \tag{19}$$

Then, the transition rate $P_{\rm tr}(E_n, E_I)$ decreases slightly faster than the exponential decay $\propto \exp(-2\frac{E_n - E_I}{\hbar\omega})$ and this fact is important for considering the nature of the sawtooth structure.

From the discussion in Sec. III, the probability weight of the nth harmonic channel $W\Psi_n(Q,t)$ can be approximated in the potential region as

$$W\Psi_n(Q,t) \equiv |C_n\Psi_n(Q,t)|^2 \sim P_{\rm tr}(n)|\Psi_{0,n}(Q)|^2, \tag{20}$$

where $\Psi_{0,n}(Q)$ is the scattering eigenstate of the unperturbed system at $E = E_n$. From the definition of the dominant harmonic channel given by Eq. (13) with Eq. (14), $|\Psi_{0,n}(Q)|^2$ with $n < \bar{n}$ is negligible in the potential region and $W\Psi_n(Q,t)$ does not practically contribute to tunneling. For $n \geqslant \bar{n}$, $W\Psi_n(Q,t)$ rapidly decreases with increasing n from Eq. (19). Therefore, the waveform in the potential region is mainly constructed by the dominant harmonic channel of $\bar{n}$ and contributions of higher harmonic channels with $n > \bar{n}$ are considerably small. When $|\Psi_{0,n}(Q)|^2 \sim O(1)$, the weight of the dominant harmonic channel is roughly approximated by the transition rate as $W\Psi_{\bar{n}}(Q,t) \sim P_{\rm tr}(\bar{n})$. Since $E_{\bar{n}} \sim V_0$ when $\hbar\omega \ll V_0$, Eq. (19) at $n = \bar{n}$ is roughly estimated as

$$\begin{aligned} P_{\rm tr}(E_{\bar{n}}, E_I) &\sim \frac{\hbar\omega}{2\pi(V_0 - E_I)} \\ &\quad \times \exp\left\{-2\frac{V_0 - E_I}{\hbar\omega}\left[\ln\left(\frac{2(V_0 - E_I)}{\epsilon V_0}\right) - 1\right]\right\} \\ &\propto \epsilon^{2\frac{V_0 - E_I}{\hbar\omega}} \quad \text{(for fixed } \hbar\omega\text{)}. \end{aligned} \tag{21}$$

This formula estimates the upper envelope of the sawtooth structure, which is proportional to the exponentiation of the base ϵ with the power $2\frac{V_0 - E_I}{\hbar\omega}$. Note that the essentially same formula is obtained by using semiclassical approximation relying on the Melnikov method in the framework of the stable-unstable manifold guided tunneling (SUMGT) for several potential models including the model under consideration [18,21,22].

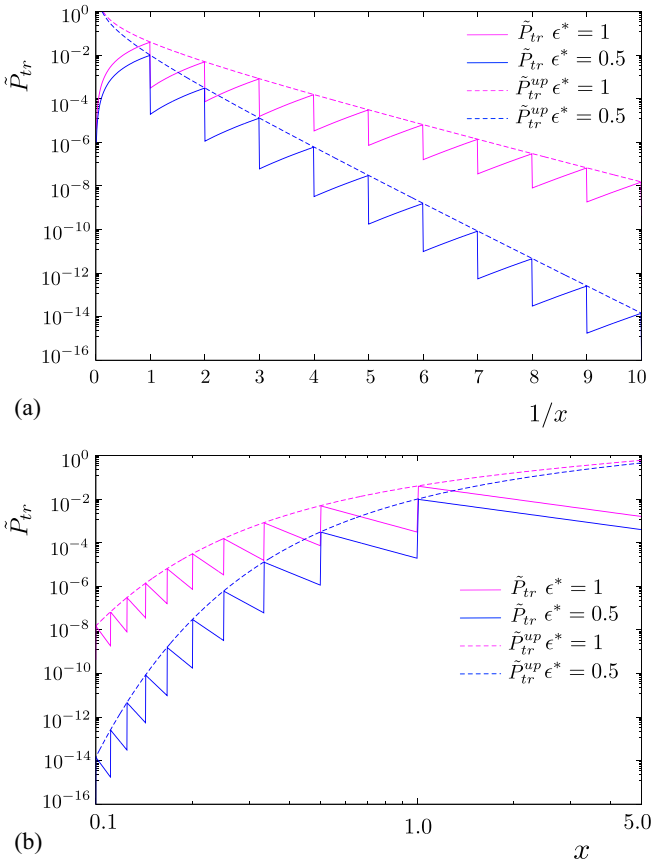

FIG. 11. Changes of $\tilde{P}_{\rm tr}(x)$ in Eq. (22) with Eq. (23) together with those of $\tilde{P}^{\rm up}_{\rm tr}$ in Eq. (24) at $\epsilon^* = 1$ and 0.5. (a) Changes with $1/x$. (b) Changes with x.

Let us estimate the transition rate $P_{\rm tr}(n)$ at $n = \bar{n}$ as a function of $\hbar\omega$, which is given by Eq. (18) combined with Eq. (13). Here, we take $x = \hbar\omega$, $\epsilon^* = e\epsilon$, $V_0 = 1$, and $E_I = 0$ for simplicity and obtain, from the second equation in Eq. (18), the transition rate for $|n| \gtrsim \frac{e\epsilon V_0}{2\hbar\omega}$ as a function of x:

$$\tilde{P}_{\rm tr}(x) = \frac{1}{2\pi n^*}\left(\frac{\epsilon^*}{2n^* x}\right)^{2n^*}, \tag{22}$$

where n^* corresponds to $\bar{n}$ in Eq. (13) and is defined as

$$n^* = \min\{n | n > 1/x\}. \tag{23}$$

Furthermore, Eq. (21) is rewritten as

$$\tilde{P}^{\rm up}_{\rm tr}(x) = \frac{x}{2\pi}\left(\frac{\epsilon^*}{2}\right)^{2/x}. \tag{24}$$

Figures 11(a) and 11(b) show the changes of $\tilde{P}_{\rm tr}$ together with those of $\tilde{P}^{\rm up}_{\rm tr}$ at $\epsilon^* = 1$, 0.5 as functions of $1/x$ and x in semilogarithmic and logarithmic scales, respectively.

Figure 11(a) corresponds to the case of changing $1/\hbar$. Namely, $\tilde{P}_{\rm tr}$ qualitatively reproduces the sawtooth structure of P_t^Q in Fig. 7 and $\tilde{P}^{\rm up}_{\rm tr}$ provides the upper envelope of $\tilde{P}_{\rm tr}$, whose slope changes with ϵ^*, because the exponential factor in Eq. (24) is expressed as a base $\epsilon^*/2$ raised to a $2/x$. In each interval between switching points, $\tilde{P}_{\rm tr}$ increases with $1/x$ as

$\propto(1/x)^{2n^*}$ and well captures the change of P_t^Q. This means that the tunneling probability in the transmissive region, P_t^Q, is not significantly influenced by resonance eigenstates. To consider the change of P_p^Q, we have to take into account the resonance effect in the potential region. Indeed, from Eq. (20), the probability density at the first resonance peak can be estimated by multiplying the probability density of the first resonance state of the unperturbed system by $P_{\rm tr}(\bar{n})$; thus its average value over the potential region should reproduce the resonance peak in P_p^Q. Due to the wide skirt of the resonance peak, P_p^Q should increase more rapidly than exponential functions of $1/\hbar$ in each interval between switching points.

Figure 11(b) corresponds to the case of changing ω: $\tilde{P}_{\rm tr}$ qualitatively reproduces the sawtooth structure of P_t^Q in Fig. 10 and $\tilde{P}_{\rm tr}^{\rm up}$ provides the upper envelope of $\tilde{P}_{\rm tr}$. The smaller ϵ^* is, the more rapidly $\tilde{P}_{\rm tr}^{\rm up}$ decreases with decreasing x because of the exponential factor $(\epsilon^*/2)^{2/x}$ in Eq. (24). In each interval between switching points, $\tilde{P}_{\rm tr}$ decreases as $\propto 1/x^{2n^*}$ with x and the slope becomes steeper with increasing n^*. Thus $\tilde{P}_{\rm tr}$ well captures the change of P_t^Q for $\omega < \omega_1^c$. The step height decreases with decreasing x, but is not negligible even at $x = 0.1$ on the logarithmic scale. To confirm this, we estimate how the step height converges in the limit of $x \to 0$, i.e., $n \to \infty$. From Eq. (23), x takes a value of $x_n^c = 1/n$ at each switching point, so that $n^* = n + 1$ at $x = x_n^c - 0$ and $n^* = n$ at $x_n^c + 0$. Then, $\tilde{P}_{\rm tr}(x)$ is represented at $x = x_n^c - 0$ and $x_n^c + 0$ as

$$\tilde{P}_{\rm tr}\left(x_n^c - 0\right) = \frac{1}{2\pi(n+1)}\left(\frac{n}{2(n+1)}\right)^{2(n+1)}, \tag{25}$$

$$\tilde{P}_{\rm tr}\left(x_n^c + 0\right) = \frac{1}{2\pi n}\left(\frac{n}{2n}\right)^{2n}. \tag{26}$$

Thus both $\tilde{P}_{\rm tr}(x_n^c - 0)$ and $\tilde{P}_{\rm tr}(x_n^c + 0)$ converge to zero in the limit of $n \to \infty$, so that the step height $\tilde{P}_{\rm tr}(x_n^c + 0) - \tilde{P}_{\rm tr}(x_n^c - 0)$ goes to zero. However, the ratio of $\tilde{P}_{\rm tr}(x_n^c - 0)$ to $\tilde{P}_{\rm tr}(x_n^c + 0)$ converges to a nonzero value as

$$\lim_{n\to\infty}\frac{\tilde{P}_{\rm tr}\left(x_n^c - 0\right)}{\tilde{P}_{\rm tr}\left(x_n^c + 0\right)} = \lim_{n\to\infty}\frac{1}{4}\left(1+\frac{1}{n}\right)^{-2n}\left(1+\frac{1}{n}\right)^{-3} = \frac{1}{4e^2}. \tag{27}$$

Hence every step has a finite height on a logarithmic scale even when n is a large integer and this seems to be true in real calculations in Figs. 7 and 10.

Finally, we mention the relation to the staircase structure reported by Hanada *et al.* [29]. When P_p^Q and P_t^Q are regarded as functions of the incident energy E_I, they form staircase structures, which are qualitatively reproduced by Eq. (18) combined with Eq. (13); for details, see Appendix B. These staircase structures are similar to those observed for a nearly integrable Hénon map [29].

VI. DISCUSSION

In this paper, we explored how tunneling probabilities change depending on either Planck's constant $\hbar$ or angular frequency ω for the periodically perturbed rounded-rectangular potential, for which instanton tunneling is substantially prohibited. As a result, we found that the sawtooth structure is attributed to the repeated replacement of the dominant harmonic channel as $1/\hbar$ or ω changes in the process of the multiquanta absorption tunneling (MQAT).

Namely, the periodic perturbation generates an energy ladder of harmonic channels at $E_n = E_I + n\hbar\omega$. Since instanton tunneling is substantially prohibited, harmonic channels with $E_n > V_0$ generate tunneling probabilities in the potential and transmissive regions in the MQAT regime of $\hbar\omega \ll V_0 - E_I$. Furthermore, the transition rates from the incident state with $E = E_I$ to harmonic channels should decay more than exponentially with E_n for $E_n > V_0$ [see Eq. (19)]; thus the harmonic channel with the lowest energy $E_{\bar{n}}$ in the range $E > V_0$ dominantly contributes to noninstanton tunneling. When the tunneling probability is written as a function of $1/\hbar$ or ω, a sudden change of the tunneling probability is observed in each neighborhood of the switching points at $E_n = V_0$ given by Eq. (15) or Eq. (16), at which the replacement of the dominant harmonic channel occurs. Namely, when the order of the dominant harmonic channel changes from $\bar{n} = n$ to $\bar{n} = n + 1$ passing through a switching point, the tunneling probability suddenly drops in its neighborhood called the transition region.

The nature of the sawtooth structure can be characterized by using the approximate formula of the transition rate $P_{\rm tr}(n)$ given by Eq. (18), which was introduced in the previous works to estimate transition rates from the incident state with $E = E_I$ to harmonic channels with $E = E_n$ for the periodically perturbed step and rectangular potentials [18,21]. Since a major part of the tunneling probability is determined by the transition rate, the change of tunneling probability in the transmissive region, P_t^Q, is qualitatively explained by Eq. (22) with Eq. (23), where the variable x is regarded as $x \propto \hbar\omega$. Furthermore, the formula (21) qualitatively estimates the upper envelope of the sawtooth structure, which is proportional to $\epsilon^{2\frac{V_0-E_I}{\hbar\omega}}$, when $\hbar\omega$ is fixed. Note that, as shown in Appendix B, the staircase structure is also observed when the incident energy E_I is changed and its feature is qualitatively explained by the approximate formula of the transition rate $P_{\rm tr}(n)$. Such a staircase structure in the tunneling probability is observed for a nearly integrable Hénon map [29].

In the potential region, a sudden change of the tunneling probability P_p^Q is also observed in each transition region. Furthermore, P_p^Q is affected by resonance eigenstates, although they do not have classical counterparts. Indeed, the first resonance peak appears at each top edge of the sawtooth structure, at which the condition $\mathrm{Re}E_1^r = E_I + \bar{n}\hbar\omega$ is satisfied and a clear resonance hump of the probability density is observed in the potential region. A clear peak does not appear at the second resonance, but a probability distribution with twin peaks is observed. The first resonance peak has a wide skirt in each interval between switching points, which makes P_p^Q grow more than exponential functions as a function of $1/(\hbar\omega)$ and hides the second resonance peak. Thus the first resonance peaks further enhance the tunneling probability in the potential region. A similar stepwise transition accompanied by resonance peaks is also observed for a periodically perturbed cubic polynomial potential [31]. In this case, MQAT induces tunneling from the potential well to the outside and the tunneling probability is enhanced when one of the harmonic

channels coincides with one of the resonance states around the threshold of the potential well.

For the continuous-time models that have a single dominant saddle in the classical phase space, MQAT is interpreted as the stable-unstable manifold guided tunneling (SUMGT) in terms of the semiclassical analysis [14–18,21,23]. Furthermore, the Melnikov method provides a formula essentially the same as Eq. (21) for several potential models [18,21,22]. Therefore, it is crucial to explore the underlying mechanism of the sawtooth structure from the viewpoint of the semiclassical analysis. We will address this issue in a forthcoming paper. Indeed, we will consider the problem of to what extent the complex semiclassical method reproduces the change of tunneling probability with $1/\hbar$ even in the situation that quantum resonance eigenstates have no classical counterparts. We will also consider the problems of how precisely the Melnikov method estimates the envelope of the sawtooth structure with $1/\hbar$ or ω and how precisely the Melnikov method estimates the power of the exponentiation of the base ϵ when $\hbar\omega$ is fixed.

For the case that the potential width is not sufficiently large, instanton tunneling becomes non-negligible and the sawtooth structure should be modified such that the slopes in transition regions become more gradual like that caused by instanton. In this case, two or more harmonic channels with energies around the threshold of the potential barrier should contribute to the tunneling process and the competition among them should affect the formation of the sawtooth structure. The tunneling for the nearly integrable Hénon map and periodically perturbed cubic polynomial potential should be categorized into this case [29,31]. A periodically perturbed Eckart potential is suitable for investigating the problem of how the sawtooth structure changes depending on the potential width due to the effect of the instantonlike tunneling working for harmonic channels below the potential height [18]. As discussed in Sec. III, the Eckart potential has no resonance eigenstates and the sawtooth structure without resonance peaks should be observed when a periodic perturbation is applied to it [30].

As mentioned in Sec. III, for tunneling processes in the MQAT regime [5,6], we assume that the transition rate $P_{\rm tr}(n)$ from the initial state to a harmonic channel is a regular function of n and the resonance eigenstates and their eigenenergies are close to those of the unperturbed system. For a system in the CAT regime, most energy levels and corresponding eigenstates are markedly different from those of classically integrable systems. Thus one needs a different scenario to treat such a tunneling process, e.g., the CAT theory.

From the discussion in Sec. III, for a system in the RAT regime [8–12], a part, at least, of energy levels and the corresponding eigenfunctions are fairly deformed from unperturbed ones. Thus, from the viewpoint of MQAT, the underlying mechanism of the tunneling process should be modified and one needs either an additional scenario or another different scenario for explaining the tunneling process, e.g., the RAT theory. It is interesting to investigate the transition in the tunneling process from a nearly integrable system with a dominant saddle and without (visible) nonlinear resonances to that with nonlinear resonance(s). The problem is how the tunneling process via nonlinear resonance(s) merges with or takes the place of that based on MQAT. If the merging scenario is true, additional peaks induced by RAT would considerably deform the base formed by MQAT, though the scenario may change depending on the situation.

Concerning the situation that a regular region formed by tori is embedded in a chaotic sea, there exists no isolated dominant saddle that separates these two regions and the scenario based on MQAT is not directly applicable to the tunneling process. When one or multiple nonlinear resonances form island chains in the regular region, the leaking rate from a quantized torus to a chaotic sea is enhanced [9–12]. When a single nonlinear resonance exists, the tunneling probability changes with $1/\hbar$ in a manner similar to the sawtooth structure caused by MQAT and resonance peaks seem to be observed when the initial state and an excited state are connected through harmonic channels via the nonlinear resonance. From the semiclassical analysis in Ref. [12], we may infer that multiple saddles caused by the nonlinear resonance play a similar role to the saddle in the MQAT regime although the situation is more complicated.

Further developments in the directions discussed above are left for future work.

ACKNOWLEDGMENT

The authors are grateful to Dr. Y. Hanada for the valuable discussion. K.I. was supported by JSPS KAKENHI Grants No. JP22H01146 and No. JP22K03476.

APPENDIX A: SCATTERING EIGENSTATES AT RESONANCE CONDITIONS

To search resonance eigenstates, we set the incident energy E_I in the range $E_I > V_0$ and see the change of P_p^Q defined by Eq. (8) with E_I at the representative values of ϵ. Figure 12(a) shows P_p^Q in the range $1.0 \leqslant E_I \leqslant 1.00015$ at $\omega = 0.3$ and $\hbar = \hbar_{\rm ref}$ for $\epsilon = 0$, 0.05, 0.1, and 0.2. For each value of ϵ, P_p^Q has a peak corresponding to the first resonance state at $E_I = {\rm Re}E_1^r \sim 1.000015$. The largest resonance peak is observed at $\epsilon = 0$ and the peaks decrease with increasing ϵ. In particular, the peaks at $\epsilon = 0.1$ and 0.2 are considerably smaller than the others. As shown in Fig. 12(b), the waveform of the first resonance state at $\epsilon = 0$ has a clear single hump in the potential region $Q_L \leqslant Q \leqslant Q_R$, while that at $\epsilon = 0.05$ has a hump accompanied by a high-frequency oscillation caused by a scattering eigenstate with higher energy. Namely, it is regarded as a superposition of the resonance eigenstate at $E_I = {\rm Re}E_1^r$ and the nearest harmonic channel at $E = {\rm Re}E_1^r + \hbar\omega$. At $\epsilon = 0.1$ and 0.2, the probability densities swell in the potential region but are irregularly deformed by more than one harmonic channel at $E = {\rm Re}E_1^r + n\hbar\omega$ $(n > 0)$.

Compared with the probability density in the MQAT regime labeled "m" in Fig. 9, where $E_I = 0.75$, $\epsilon = 0.2$, and $\hbar = 1.006\hbar_{\rm ref}$, the probability density at $\epsilon = 0.2$ is apparently irregular. In the MQAT regime, harmonic channels with $E = E_{\bar{n}} + l\hbar\omega$ $(l > 0)$ are more than exponentially small compared with the dominant channel with $E = E_{\bar{n}}$ because the transition rate $P_{\rm tr}(n)$ decreases more than exponentially with n. Thus the second dominant channel with $E = E_{\bar{n}} + \hbar\omega$ merely makes a small additional contribution to forming a wave function in the

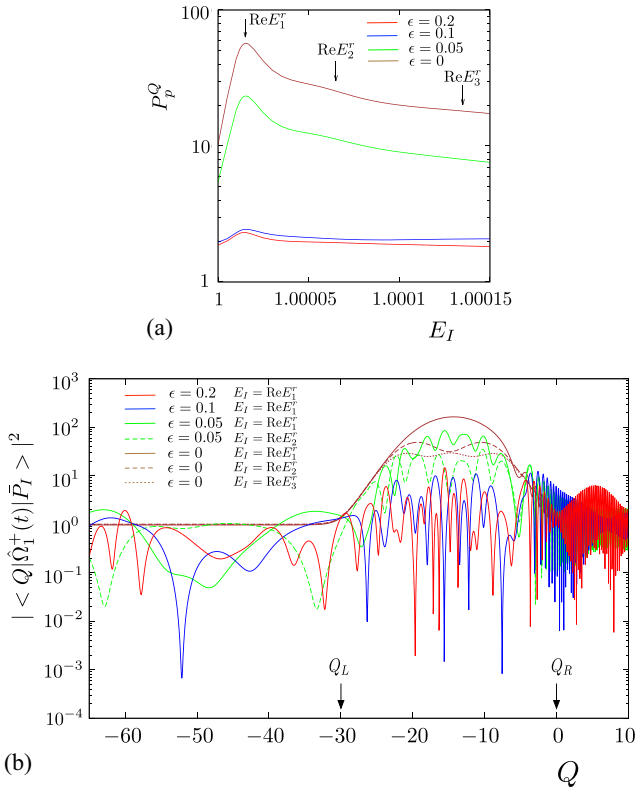

FIG. 12. Resonance eigenstates in the range $E_I > V_0$ at $\omega = 0.3$ and $\hbar = \hbar_{\mathrm{ref}}$ for $\epsilon = 0$, 0.05, 0.1, and 0.2. (a) Changes of P_p^Q with E_I. The first resonance peak is observed at $\mathrm{Re}E_1^r \sim 1.000015$ and the positions of the second and third resonance peaks are estimated as $\mathrm{Re}E_1^r \sim 1.000065$ and $\mathrm{Re}E_1^r \sim 1.000135$, respectively. (b) Probability densities of resonance eigenstates.

potential regime. On the other hand, for the case of $E_I > V_0$, the transitions to multiple harmonic channels around the incident energy E_I occur in a classically accessible region. Indeed, the transition rates from the incident state to those harmonic channels take values of the order of ϵ. They markedly disturb the first resonance state waveform at $E_1^r = E_I$ when ϵ is not negligibly small.

As shown in Fig. 12(a), no clear peaks are observed at the positions of the second and third resonances because the wide skirt of the first resonance peak spreads over the right-hand side and hides their existence even for the unperturbed system at $\epsilon = 0$. For the cases of $\epsilon = 0$ and 0.05, small humps corresponding to the second resonance are however observed near the position labeled $\mathrm{Re}E_2^r \sim 1.000065$. Actually, as shown in Fig. 12(b), for the case of $\epsilon = 0$, a hump accompanied by twin peaks, which is regarded as a superposition of the first and second resonance states, is observed. For the case of $\epsilon = 0.05$, the twin peaks deformed by the harmonic channel at $E = \mathrm{Re}E_1^r + \hbar\omega$ are observed. However, for the cases of $\epsilon = 0.1$ and 0.2, no clear twin peaks are observed due to the disturbance by multiple harmonic channels. Furthermore, for the case of $\epsilon = 0$, a hump with triple peaks corresponding to the third resonance state is observed at $E = \mathrm{Re}E_3^r \sim 1.000135$.

Note that, at $\epsilon = 0$, the probability densities take almost the same values independent of E_I in the transmissive region. This means that the resonance eigenstates do not influence the probability density in the transmissive region, but this fact does not contradict the fact that the resonance eigenstates have long lifetimes and rather allows them to do so because of relatively smaller leak rates.

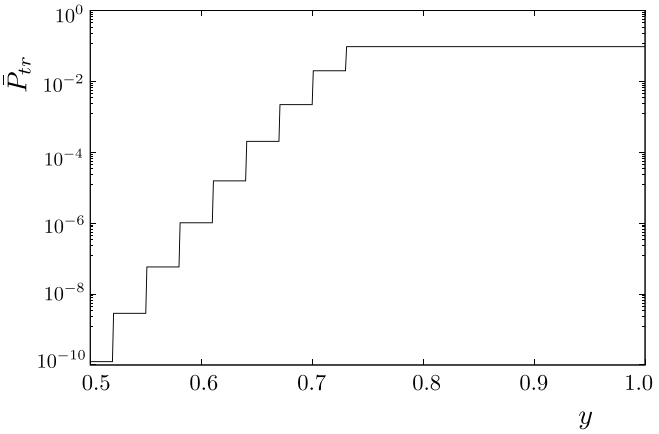

FIG. 13. Change of $\bar{P}_{\mathrm{tr}}(x)$ in Eq. (B1) with Eq. (B2) at $c = 0.03$ and $\epsilon = 0.2$.

APPENDIX B: CHANGE OF TUNNELING PROBABILITIES WITH THE INITIAL ENERGY E_I

Here, we regard the transition rate approximately given by Eq. (18) with Eq. (13) as a function of E_I when $\hbar$, ω, and ϵ are fixed. Setting up as $y = E_I < 1$, $V_0 = 1$, and $c = \hbar\omega < \epsilon < 1$, Eq. (18) can be rewritten as

$$\bar{P}_{\mathrm{tr}}(y) = \min\left\{\frac{1}{2\pi n^{**}}\left(\frac{\mathrm{e}\epsilon}{2n^{**}c}\right)^{2n^{**}}, \frac{2c}{\pi\epsilon}\right\}, \tag{B1}$$

where n^{**} corresponding to $\bar{n}$ is defined as

$$n^{**} = \min\{n | n \geqslant (1-y)/c\}. \tag{B2}$$

Figure 13 shows the change of $\bar{P}_{\mathrm{tr}}(y)$ at $c = 0.03$ and $\epsilon = 0.2$. For $n^{**} \gtrsim \frac{\mathrm{e}\epsilon}{2c}$, i.e., $y \lesssim 1 - \frac{\mathrm{e}\epsilon}{2} \sim 0.728$, $\bar{P}_{\mathrm{tr}}(y)$ forms a staircase function owing to the stepwise change of n^{**} with y. When $|n^{**}| \lesssim \frac{\mathrm{e}\epsilon}{2c}$, i.e., $y \gtrsim 1 - \frac{\mathrm{e}\epsilon}{2}$, $\bar{P}_{\mathrm{tr}}(y)$ takes a constant value of $\frac{2c}{\pi\epsilon} \sim 0.0955$. But, in the range $|n| \lesssim \frac{\mathrm{e}\epsilon}{2c}$, real transition rates do not take a constant value and rather undulate accompanied by dips at some values in n, at which the transition from the initial state with $E = E_I$ to the harmonic channel with $E = E_I + n\hbar\omega$ is extremely suppressed [18,21]. Furthermore, since the probability density is estimated as Eq. (20), P_p^Q is affected by resonance eigenstates at the condition $\mathrm{Re}E_m^r = E_I + n\hbar\omega$ even in the range $|n| \lesssim \frac{\mathrm{e}\epsilon}{2c}$.

Figure 14 shows changes of P_p^Q and P_t^Q with E_I at $\epsilon = 0.2$, $\omega = 0.3$, and $\hbar = \hbar_{\mathrm{ref}}$. There exists a threshold energy E^{cl} such that, for the range $E_I < E^{\mathrm{cl}}$, any classical particles are forbidden to reach the transmissive region and purely quantum tunneling occurs. Note that E^{cl} is larger than $V_0 - \epsilon$ ($> V_0 - \frac{\mathrm{e}\epsilon}{2}$). Thus P_t^Q forms a staircase structure in the range $E_I < E^{\mathrm{cl}}$, which is qualitatively reproduced by that in Fig. 13. This staircase structure is similar to that of the nearly integrable Hénon map studied by Hanada *et al.* [29], though they took the quantum number of the initial state instead of the incident energy E_I as the control parameter. In each unit of

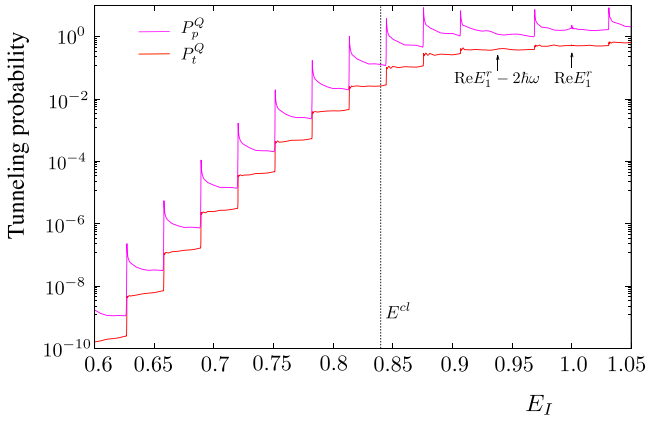

FIG. 14. Changes of P_p^Q and P_t^Q as functions of the incident energy E_I at $\epsilon = 0.2$, $\omega = 0.3$, and $\hbar = \hbar_{\mathrm{ref}}$. In the range $E_I < E^{\mathrm{cl}} \sim 0.83985$, any classical particles are forbidden to reach the transmissive region.

the staircase structure, P_t^Q is almost constant as long as $\bar{n}$ is the same. On the other hand, P_p^Q has resonance peaks at $E_I = \mathrm{Re}E_1^r - \bar{n}\hbar\omega$, each of which has a wide skirt on the right-hand side of it.

Even in the range $E_I > E^{\mathrm{cl}}$, staircase structures still exist in P_p^Q and P_t^Q, although the heights of steps become smaller. Furthermore, P_p^Q is accompanied by resonance peaks. As shown in Fig. 12 in Appendix A, P_p^Q merely has a very small resonance peak at $E_I = \mathrm{Re}E_1^r$ due to the disturbance by harmonic channels with $E_n = \mathrm{Re}E_1^r + n\hbar\omega$, with $n \geqslant 1$, and P_t^Q does not have a clear step. However, the other peaks of P_p^Q at $E_I = \mathrm{Re}E_1^r - \bar{n}\hbar\omega$, except $\bar{n} = 2$, are larger than that at $E_I = \mathrm{Re}E_1^r$. It means that the contributions of harmonic channels at $E_n = E_I + n\hbar\omega$ with $n \neq \bar{n}$ are relatively small. At $E_I = \mathrm{Re}E_1^r - 2\hbar\omega$ ($\bar{n} = 2$), P_p^Q has no clear peak and P_t^Q has no clear step. We suspect that the transition to the resonance eigenstate at $E = \mathrm{Re}E_1^r$ is substantially forbidden due to a dip in the transition rate.

[1] *Tunneling in Complex Systems*, edited by S. Tomsovic (World Scientific, Singapore, 1998).

[2] J. Ankerhold, *Quantum Tunneling in Complex Systems The Semiclassical Approach* (Springer-Verlag, Berlin, 2007).

[3] *Dynamical Tunneling: Theory and Experiment*, edited by S. Keshavamurthy and P. Schlagheck (CRC Press, Boca Raton, FL, 2011).

[4] M. J. Davis and E. J. Heller, J. Chem. Phys. **75**, 246 (1981).

[5] W. A. Lin and L. E. Ballentine, Phys. Rev. Lett. **65**, 2927 (1990).

[6] O. Bohigas, S. Tomsovic, and D. Ullmo, Phys. Rep. **223**, 43 (1993); S. Tomsovic and D. Ullmo, Phys. Rev. E **50**, 145 (1994).

[7] C. Dembowski, H.-D. Gräf, A. Heine, R. Hofferbert, H. Rehfeld, and A. Richter, Phys. Rev. Lett. **84**, 867 (2000); W. K. Hensinger *et al.*, Nature (London) **412**, 52 (2001); D. A. Steck, W. H. Oskay, and M. G. Raizen, Science **293**, 274 (2001).

[8] O. Brodier, P. Schlagheck, and D. Ullmo, Phys. Rev. Lett. **87**, 064101 (2001); Ann. Phys. (NY) **300**, 88 (2002).

[9] S. Löck, A. Bäcker, R. Ketzmerick, and P. Schlagheck, Phys. Rev. Lett. **104**, 114101 (2010).

[10] A. Bäcker, R. Ketzmerick, and S. Löck, Phys. Rev. E **82**, 056208 (2010).

[11] N. Mertig, J. Kullig, C. Löbner, A. Bäcker, and R. Ketzmerick, Phys. Rev. E **94**, 062220 (2016).

[12] F. Fritzsch, A. Bäcker, R. Ketzmerick, and N. Mertig, Phys. Rev. E **95**, 020202(R) (2017).

[13] K. Takahashi and K. S. Ikeda, Ann. Phys. (NY) **283**, 94 (2000).

[14] K. Takahashi and K. S. Ikeda, J. Phys. A: Math. Gen. **36**, 7953 (2003).

[15] K. Takahashi and K. S. Ikeda, Europhys. Lett. **71**, 193 (2005); **75**, 355(E) (2006); J. Phys. A: Math. Theor. **41**, 095101 (2008).

[16] K. Takahashi and K. S. Ikeda, Phys. Rev. A **79**, 052114 (2009).

[17] K. Takahashi and K. S. Ikeda, J. Phys. A: Math. Theor. **43**, 192001 (2010).

[18] K. Takahashi and K. S. Ikeda, Phys. Rev. E **86**, 056206 (2012).

[19] L. S. Schulman, *Techniques and Applications of Path Integration* (Wiley, New York, 1981).

[20] W. H. Miller, J. Chem. Phys. **53**, 1949 (1970); Adv. Chem. Phys. **25**, 69 (1974).

[21] K. Takahashi and K. S. Ikeda, Phys. Rev. E **84**, 026203 (2011).

[22] K. Takahashi, J. Phys. A: Math. Theor. **54**, 475701 (2021).

[23] K. Takahashi and K. S. Ikeda, Phys. Rev. Lett. **97**, 240403 (2006); **107**, 219903(E) (2011).

[24] M. Wilkinson, Physica D **21**, 341 (1986).

[25] S. C. Creagh and N. D. Whelan, Phys. Rev. Lett. **84**, 4084 (2000).

[26] S. C. Creagh, Nonlinearity **17**, 1261 (2004); **18**, 2089 (2005); C. S. Drew, S. C. Creagh, and R. H. Tew, Phys. Rev. A **72**, 062501 (2005).

[27] A. Shudo, Y. Hanada, T. Okushima, and K. S. Ikeda, Europhys. Lett. **108**, 50004 (2014).

[28] Y. Hanada, A. Shudo, and K. S. Ikeda, Phys. Rev. E **91**, 042913 (2015).

[29] Y. Hanada, A. Shudo, T. Okushima, and K. S. Ikeda, Phys. Rev. E **99**, 052201 (2019).

[30] K. Takahashi (unpublished). For the periodically perturbed step potential, sawtooth structures without resonance peaks are observed, since it has no resonance states.

[31] T. Oya and K. S. Ikeda, Global I-NI transition caused by tunnel stair-like structure (in Japanese) (unpublished).

[32] K. Takahashi and K. S. Ikeda, J. Chem. Phys. **106**, 4463 (1997).

[33] M. Büttiker and R. Landauer, Phys. Rev. Lett. **49**, 1739 (1982); Phys. Scr. **32**, 429 (1985).

[34] M. Abramowitz and I. A. Stegun, *Handbook of Mathematical Functions* (Dover Publications, New York, 1965).